Journal of the Korean Nuclear Society
Volume 33, Number 2, pp.209~224, April, 2001

Development of a System Analysis Code, SSC-K, for Inherent Safety Evaluation of The Korea Advanced Liquid Metal Reactor

Young Min Kwon, Yong Bum Lee, Won Pyo Chang, Dohee Hahn, and Kyung Doo Kim
Korea Atomic Energy Research Institute
150 Dukjin-dong, Yusong-gu, Taejon 305-353, Korea
ymkwon@kaeri.re.kr

(Received September 21, 2000)

Abstract

The SSC-K system analysis code is under development at the Korea Atomic Energy Research Institute (KAERI) as a part of the KALIMER project. The SSC-K code is being used as the principal tool for analyzing a variety of off-normal conditions or accidents of the preliminary KALIMER design. The SSC-K code features a multiple-channel core representation coupled with a point kinetics model with reactivity feedback. It provides a detailed, one-dimensional thermal-hydraulic simulation of the primary and secondary sodium coolant circuits, as well as the balance-of-plant steam/water circuit. Recently a two-dimensional hot pool model was incorporated into SSC-K for analysis of thermal stratification phenomena in the hot pool. In addition, SSC-K contains detailed models for the passive decay heat removal system and a generalized plant control system. The SSC-K code has also been applied to the computational engine for an interactive simulation of the KALIMER plant.

This paper presents an overview of the recent activities concerned with SSC-K code model development. This paper focuses on both descriptions of the newly adopted thermal hydraulic and neutronic models, and applications to KALIMER analyses for typical anticipated transients without scram.

Key Words : system analysis code, SSC-K, liquid metal reactor, safety analysis, KALIMER

1. Introduction

The Korea Atomic Energy Research Institute (KAERI) is developing a conceptual design of KALIMER (Korea Advanced LIquid MEtal Reactor) [1], which is a sodium cooled, 150 MWe, pool-type reactor. The primary heat transport system (PHTS) of KALIMER is submerged in a big sodium pool, which provides the large thermal inertia of the system. KALIMER, with a metallic fueled core, is designed in such a way that an intrinsic negative reactivity feedback effect is expected during the anticipated transients without scram (ATWS) conditions. KALIMER features such safety systems

as a self-actuated ultimate shutdown system (USS), and gas expansion module (GEM) in the core. In a rare event that the intermediate heat transport systems (IHTS) become unavailable during power operation, the passive decay heat removal system (PSDRS) is designed to remove the core heat by natural circulation of air around the containment vessel.

The SSC-K [2] code is being developed for assessment of the inherent safety features in the KALIMER conceptual design. The SSC-K development aims at not only extensive analysis capability and flexibility, but also efficient running fast enough to simulate long transients in a reasonable amount of computer time. The code thus becomes capable of handling a wide range of transients, including normal operational transients, shutdown heat removal transients, and hypothetical ATWS events. The SSC-K code is currently being used as the main tool for system transient analysis in the KALIMR development project. This paper primarily focuses on both descriptions of the newly adopted thermal hydraulic and neutronic models, and applications to KALIMER analyses for typical ATWS events.

2. General Description of SSC-K

The SSC-K development is based on the methods and models of SSC-L [3], as its parent code, that was originally developed at Brookhaven National Laboratory to analyze loop-type liquid metal reactor (LMR) transients. Because of the inherent difference between the pool and loop designs, major modifications to the SSC-L were made in order to analyze a pool-type reactor. Now, the SSC-K code is capable of analyzing both LMR designs, loop and pool type reactors. Additional developments in the SSC-K code were made on the models for reactivity feedback effects with the metallic fuel, and the PSDRS. Recently, a

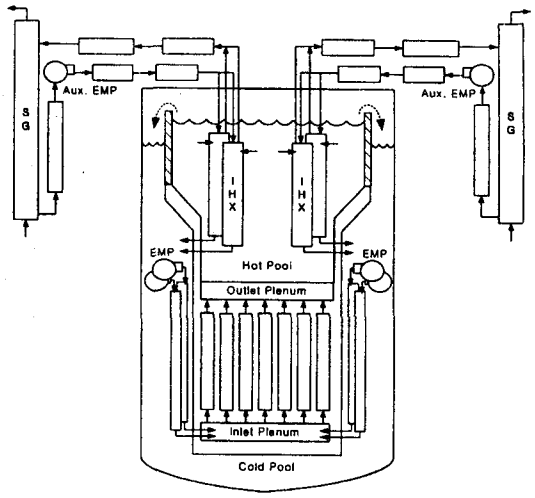

Fig. 1. SSC-K Modeling for the KALIMER Plant

two dimensional hot pool model has also been employed into SSC-K for realistic analysis of the thermal stratification phenomenon in the hot pool. The model for the control system in SSC-K is flexible enough to handle any types of control systems. For code maintenance and readability, SSC-K was converted to FORTRAN 90 free format and the use of standard FORTRAN 90 has enhanced code portability. Now, SSC-K version 0 is available and maintained in the PC/Windows environment. The SSC-K code may also be applied to the computational engine for an interactive simulation of the KALIMER plant.

2.1. Pool Thermal Hydraulic Model

2.1.1. Flow Equations

The SSC-K code simulates multiple heat transport system modules and associated controllers. A full plant model for SSC-K is used to represent KALIMER as shown in Fig.1, where several major components are represented. Each PHTS is represented with the reactor vessel flow passages, the primary pump, and the shell side of

the intermediate heat exchanger (IHX). On the other hand, each IHTS is represented with the tube side of the IHX, piping, the shell side of the steam generator (SG), and the intermediate pump. A major modification of SSC-K was made in order to represent the thermal hydraulic behaviors in the pool. In KALIMER, both the hot and cold pools have free surfaces and there is direct mixing of the coolant with these open pools prior to entering the next component. Therefore, at least two different flows would have to be modeled to characterize the coolant dynamics of the primary system. The flow from the pump to core inlet plenum would respond to the pump head and pressure losses in that circuit. The volume-averaged momentum equations for pump outlet flow (W_p) in each path can be written as follows:

$$\frac{dW_p(k)}{dt}\sum_{p}\frac{L(k)}{A(k)} = P_{Po}(k) - P_{Rin} - \sum \Delta P_{f,g}(k), \quad k = 1,\cdots,N_{path} \tag{1}$$

KALIMER has four flow paths (N_{path} = 4) in the PHTS. In the above equation, L and A means the average length and area of each flow path, respectively. The last term on the right hand side of Eq. (1) represents the pressure losses due to friction and geometric change. The pump exit pressure, P_{po}, is the sum of the pump inlet pressure and the pump head. The core inlet pressure, P_{Rin}, is obtained from a complicated algebraic equation derived by mass and momentum conservation at the core inlet plenum as follows:

$$\sum_{k=1}^{N_{path}}\frac{dW_p(k)}{dt} = \sum_{j=1}^{N_{ch}}\left\{\frac{P_{Rin} - P_{Ro} - \sum\left(\Delta P_{f,g}\right)_j}{\left(\sum L/A\right)_j}\right\} \quad j = 1,\cdots,N_{ch} \text{ and } k = 1,\cdots,N_{path} \tag{2}$$

where the core flow is expressed in terms of channel flows. The KALIMER core, schematically shown in Fig.1, is modeled with seven channels (N_{ch} = 7). The core outlet pressure, P_{Ro}, is obtained from the static head of the hot pool above core outlet elevation.

The IHX flow (W_{IHX}) would respond to the level difference between the two pools, as well as losses and gravity gains in the IHX. The volume-averaged momentum equations for IHX flow is:

$$\frac{dW_{IHX}(k)}{dt}\sum_{k}\frac{L(k)}{A(k)} = P_{Xin} - P_{Xo} - \sum \Delta P_{f,g}(k), \quad k = 1,\cdots,N_{path} \tag{3}$$

The IHX inlet pressure, P_{Xin}, is obtained from the static head between the hot pool level and the IHX inlet elevation and the IHX exit pressure, P_{Xo}, is the static head between the cold pool level and the IHX exit elevation.

The only primary piping used in KALIMER is from the discharge side of the pump to the core inlet plenum. Pipe rupture can happen in the pump discharge line. When the pipe break occurs, an additional equation is needed to describe the break flow. The external pressure for the break corresponds to the static head of the cold pool. This pressure acts as the back pressure opposing the flow out of the break. The value of this pressure is much larger than that for a loop-type design, which is generally equal to atmospheric pressure until the sodium in the guard vessel covers the break location. This makes the pipe break in a pool-type design less severe relative to a loop-type design.

2.1.2. Liquid Level in the Pool

The reactor vessel contains basically the entire inventory of the primary sodium coolant in the pool-type design. A vertical wall, called a reactor baffle, divides the primary pool into hot and cold pools as shown in Fig.1. The liquid levels in the cold and hot pools can be obtained by mass

balance at each pool. The change rate of total sodium mass in the cold pool is given from the mass balance in the cold pool:

$$\frac{d}{dt}(\rho V)_{CP} = \sum_{k=1}^{N_{path}} W_{IHX}(k) - \sum_{k=1}^{N_{path}} W_P(k) + W_{over} + W_{break} \quad (4)$$

Note that the break flow, W_{break}, is zero for an intact system and overflow from the hot pool, W_{over}, is zero if the hot pool level is below top of the reactor baffle. The cold pool level can then be obtained from the sodium mass in the cold pool by assuming that the cold pool can be represented by two distinct regions with different cross-sectional areas. Those areas are the annulus between the reactor baffle and the reactor vessel, and the average lower core region.

The change rate of the sodium mass in the hot pool is obtained from mass balance at the hot pool.

$$A_{HP}\frac{d}{dt}(\rho Z)_{HP} = W_C - \sum_{k=1}^{N_{path}} W_{IHX}(k) - W_{over} \quad (5)$$

Eq. (5) assumes that all the level changes likely to occur during the transient are confined to a constant cross-sectional area. When Eqs. (4) and (5) are solved simultaneously with the flow equations, the sodium levels for the hot and cold pools during the transient can be obtained.

2.1.3. Energy Balance in the Pool

Thermal stratification may occur in the hot pool region if the entering coolant is colder than the existing hot pool coolant and the flow momentum is not sufficient enough to overcome the negative buoyancy force. Since the fluid of the hot pool enters the IHXs, the temperature distribution of the hot pool can alter the overall system response. Hence, it is necessary to predict the hot pool temperature distribution with sufficient accuracy to determine the inlet temperature conditions for the

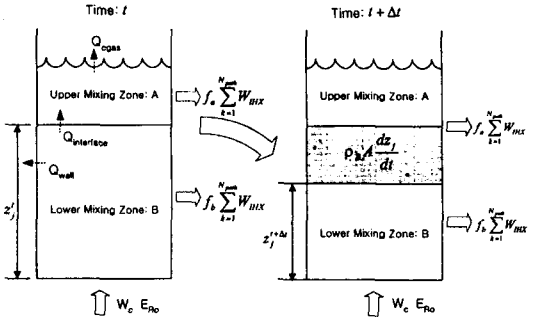

Fig. 2. The Two Mixing Zone Model for a Hot Pool

IHXs and its contribution to the net buoyancy head.

During a normal reactor scram, heat generation is reduced almost instantaneously while the coolant flow rate follows the pump coastdown. This mismatch of power-to-flow results in a situation where the temperature of the core flow entering the hot pool is lower than that of the bulk pool sodium, which leads to stratification when the coolant momentum is insufficient.

The stratification phenomenon in the hot pool is represented with the two-zone model. The hot pool is divided into two perfectly mixing zones determined by the maximum penetration distance of the core flow. This penetration distance, Z_j, is a function of the Froude number with respected to the average core exit flow. The two-zone model used in the original SSC-L code has been modified as shown in Fig. 2. A term, whose term is represented in Eqs. (6) and (7), corresponding to the change rate of energy due to the interface movement is added to the energy balance equations in the SSC-K code to make energy conserved. The temperature of each zone is computed from energy balance consideration. The temperature of the upper portion, T_A, will be relatively unchanged; in the lower region, however, T_B, will be changed and somewhat between the core exit temperature and the upper

zone temperature due to active mixing with core exit flow as well as heat transfer with the upper zone. The temperature of the upper zone is mainly affected by interfacial heat transfer. The energy conservation equation is combined with the mass conservation equation and the resultant equation yields the nonconservative form of the energy equation for lower and upper mixing zones, respectivly: The non-conservative forms of energy balance equations that determine the various temperatures in the hot pool are given below:

$$(\rho V)_A \frac{dE_A}{dt} = \begin{cases} -Q_{wall} - Q_{cgas} + Q_{interface} & \text{if} \frac{dz_j}{dt} > 0 \\ -\frac{dz_j}{dt}\rho_B A(E_B - E_A) - Q_{wall} - Q_{cgas} + Q_{interface} & \text{if} \frac{dz_j}{dt} \le 0 \end{cases} \quad (6)$$

$$(\rho V)_B \frac{dE_B}{dt} = \begin{cases} \frac{dz_j}{dt}\rho_A A(E_A - E_B) + W_C(E_{Ro} - E_B) - Q_{wall} - Q_{interface} & \text{if} \frac{dz_j}{dt} > 0 \\ W_C(E_{Ro} - E_B) - Q_{wall} - Q_{interface} & \text{if} \frac{dz_j}{dt} \le 0 \end{cases} \quad (7)$$

Currently, perfect mixing of the IHX flow with cold pool sodium is assumed. The energy balance equation for the cold pool is derived as:

$$(\rho V)_{cp} \frac{dh_{cp}}{dt} = \sum_{N_{path}} W_{IHX} h_{IHX} - h_{cp} \sum_{N_{path}} W_{IHX} + W_{over} h_{hp} - W_{over} h_{cp} + \sum_{N_{path}} W_{break} h_{break} - h_{cp} \sum_{N_{path}} W_{break} \quad (8)$$

2.1.4. Two-Dimensional Hot Pool Model

The previous two-zone model is only applicable to very slow transitions or steady state conditions. A two-dimensional hot pool model [4] has been developed to calculate the coolant temperature and velocity profiles in the hot pool. The solution domain is divided into a finite number of quadrilateral control volumes and the discretization of the governing equation is performed following the finite volume approach. The convection terms are approximated by a higher-order bounded scheme HLPA developed by Zhu [5] and the unsteady terms are treated by the backward differencing scheme.

Heat transfer to the wall of the pool is calculated along the wall surface. The governing equations for conservation of mass, momentum, energy, and both turbulent kinetic energy and the rate of turbulent kinetic energy dissipation for the κ-ε turbulence model are made in a generalized coordinate system. The SIMPLEC [6] algorithm is used for pressure-velocity coupling, where the momentum equations are implicitly solved at cell-centered locations. After validation of the stand-alone version of the two-dimensional pool model against the sample problem, it has been coupled with the SSC-K code. Users can select the two-dimensional model or the two-mixing zone model for hot pool simulation. Fig. 3 shows a sample result predicted by the two-dimensional model, which is a transient of sodium temperature distribution in the KALIMER hot pool during an initial 200 seconds for a 10 cent reactivity insertion event without scram.

2.1.5. Core Thermal Hydraulic Model

The SSC-K core region is divided into parallel channels, and each one represents a subassembly or a group of similar subassemblies. The whole length of a subassembly, from coolant inlet to coolant outlet, is represented by a channel. Usually an average rod within a subassembly is modeled, but it is possible to represent a hot subassembly instead. The flow splits among the channels are

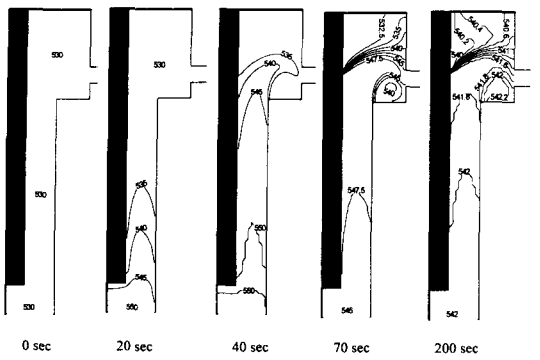

Fig. 3. Temperature Distribution Predicted by the Two-Dimensional Hot Pool Model for a 10 Cent UTOP Event

adjusted at each time step to account for the friction factor and pressure drop changes. Friction factors in the hydraulic equations are continuously updated. They account for the transition from laminar to turbulent flow in all parts of the sodium system. Reverse flow in the channels can be handled. Natural circulation also takes into account thermally driven density changes in all parts of the primary, intermediate and water/steam loops with elevation changes.

Fig. 4 shows the node structure to represent the KALIMER fuel channel. The general form of the SSC-K core channel is composed of up to five axial regions: lower plenum, lower blanket, active fuel, upper blanket, and upper plenum. Some of these regimes may be omitted at the user' s request, but the sequence should be maintained. Each axial segment is divided radially into several sections that represent fuel, gap, clad, sodium coolant, and structure sections. Axial heat conduction is neglected. Thermal expansions are accounted for in the fuel and clad, but those of the coolant channel flow area or the structure are not considered for steady-state and transient calculations. Heat transfer across the gap is modeled in terms of gap conductance. The gap conductance is computed if the gap is of finite

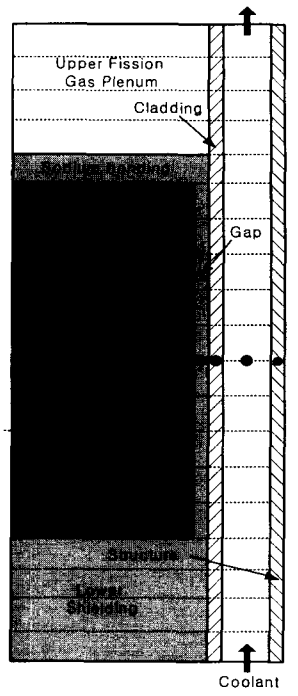

Fig. 4. Core Channel Node Structure

size; however, for a closed gap the conductance is user input.

Thermal power generation is represented by point neutron kinetics and decay heat equations. SSC-K uses a decay heat treatment similar to that normally used for delayed neutron precursors. Up to six decay heat precursor groups are used, each with its own yield and decay constant. A specified fraction of the total reactor power is generated in fuel, cladding, blanket and sodium. The axial variation of power generation is specified by a profile supplied by the user. Any power deposited in the cladding, coolant, or structural material is assumed to be distributed uniformly in the radial direction.

2.2. Reactivity and GEM Models

The SSC-L code was originally developed to analyze oxide fuel LMRs. To facilitate modeling of the metallic fuel used in KALIMER, several

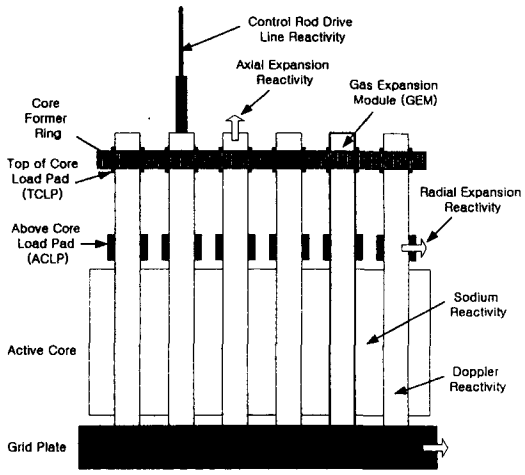

Fig. 5. Reactivity Components in a Metallic Fueled Core

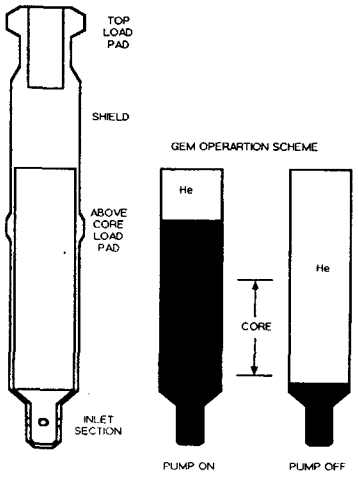

Fig. 6. Schematic of GEM Operation

modifications have been made for the SSC-K code. For neutronic calculations, SSC-K uses the point kinetics equations with detailed reactivity feedback from each channel. Reactivity effects are required both for transient safety analysis and for control requirements during normal operation. Reactivity feedback models have been developed for SSC-K in order to account for the effects due to Doppler, sodium density/void, fuel axial expansion, core radial expansion and control rod driveline expansion. Fig. 5 shows the components of reactivity feedback considered in the KALIMER core.

In addition to the reactivity model, a GEM model has been developed for SSC-K. The GEM assemblies are added to KALIMER core in order to supplement the negative reactivity feedback once the pump is tripped. Fig. 6 depicts the operation scheme of the GEM. When the pumps trip and the pressure drops, the sodium within the GEMs at the active core elevation is displaced by expanding helium gas, thus increasing the leakage of neutrons from the core. Currently, the sodium density inside the GEM is assumed to be the axial average of the neighboring channels. A sensitivity study is needed to investigate the effect of sodium density on the sodium level. If needed, the GEM model will be modified so that the axial sodium density can be calculated considering inter-assembly heat transfer. The temperature of the GEM gas is assumed to be the average of the structural temperature of neighboring channels. It is noted that improvement of the current GEM model can also be made by calculating the GEM gas temperature with taking account of the inter-assembly heat transfer. Detail description of the reactivity models and GEM model for the metallic fueled core is presented in References [7] and [8].

2.3. Passive Decay Heat Removal System Model

PSDRS is a heat removal feature in the KALIMER design that is characterized to cool the containment outer vessel with atmospheric air in a passive manner. Fig. 7 exhibits the schematic of PSDRS. The gap between the reactor vessel and the containment vessel is filled with argon gas and thus radiation heat transfer prevails due to the high temperature of these walls. Atmospheric air comes in from the inlets located at the top of the containment, and flows down through the annulus

gap between the air separator and the concrete silo. It then turns back upward passing through the other annulus gap between the containment outer surface and the air separator, and finally flows out through the stack with raised temperature by the energy gained from cooling of the containment vessel. The air flow rate is determined from various parameters. The air temperature difference between the two annulus channels, flow path or pressure drop of an orifice placed for flow control, and friction exerted on the surfaces are the main parameters affecting the flow rate.

The significance of PSDRS in the KALIMER design is that it plays a role of the only heat removal system in a total loss of heat sink accident. For this reason, its function is crucial to prevent core damage, so that performance analysis as well as realistic modeling of the system might be a key issue to provide essential knowledge for a safety evaluation of the KALIMER design. The PSDRS model [9, 10] was developed to predict the heat removal rate by this system. The model calculates not only energy balances by the heat transfers between the walls, but also the air flow rate driven by gravitational force between the air flow channels to estimate the heat removal rate. Non-linear differential equations are solved using the Runge-Kutta method while the air temperature profile is obtained from theoretical manipulation. The PSDRS model has been connected to the SSC-K code, and the present model will be continuously improved through more rigorous theoretical bases.

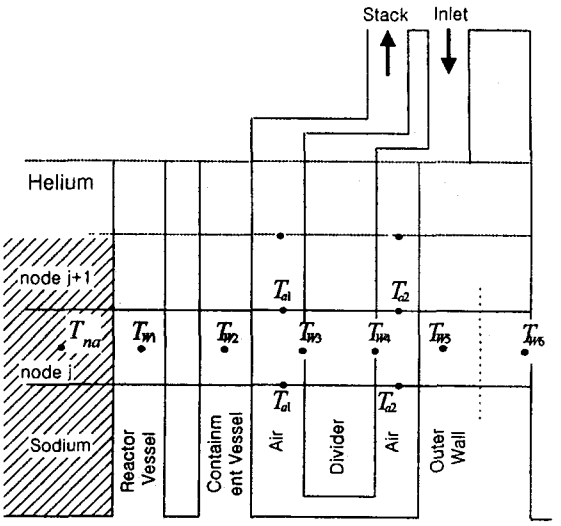

Fig. 7. PSDRS Model

2.4. IHTS and Steam Generation System Models

The representation of the IHTS and steam generation system in the SSC-K code is handled within the MINET [11] package, which is coupled and interfaced to SSC-L. The MINET package is a computer code developed for the transient analysis of intricate fluid flow and heat transfer networks, such as those found in the balance-of-plant in power generation facilities. It can be utilized as a stand-alone code, or interfaced with another computer code. The SSC-K code coupling with MINET can fully represent the thermal hydraulic system such as pipes, pumps, heat exchangers, valves, etc., thereby reducing the need for estimating essential transient boundary conditions. SSC-L/MINET has been applied to analyses of the Clinch River Breeder Reactor (CRBR) and the Japanese MONJU plants. Most of MINET portion except some heat transfer correlations for the helical coil steam generator remains in the SSC-K code development without further modification.

2.5. KALIMER Plant Analyzer

The conventional method to handle the code output is not convenient for analysis because of text-oriented programming. The plant analyzer using a graphical interface makes it possible to analyze the simulation results while the code is

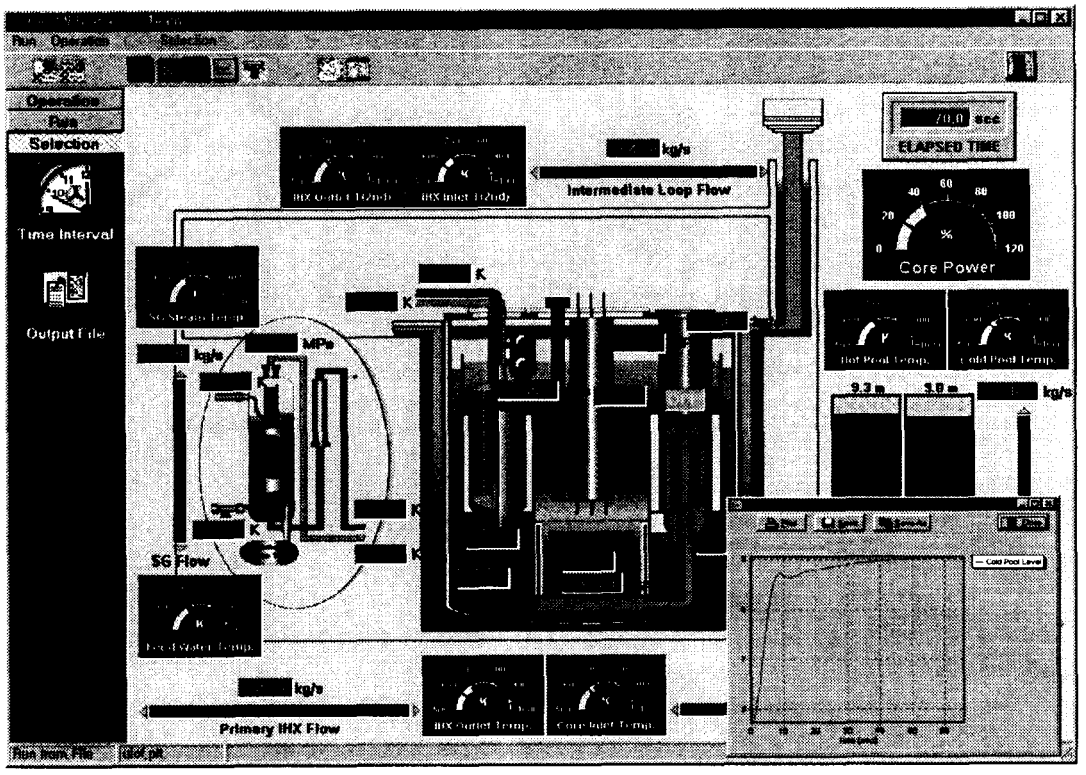

Fig. 8. KALIMER Plant Mimic of NPA4K

executing. The Nuclear Plant Analyzer for KALIMER (NPA4K) [12] was developed using Delphi program language in the PC/Windows environment. The SSC-K code can be executed within the NPA4K mode and all the key parameters are displayed in either text or graphical forms. The user dialog box to select the variables for the X-Y plot is provided and the coordinates for the selected plots are modified dynamically with simulation time. The live system variable plots and live graphic depictions of the plant state help the user to understand the system behavior. The user may interrupt and resume a transient simulation at any time, examine the plant parameters, make changes, take manual actions and initiate malfunctions. Fig. 8 indicates a mimic of the KALIMER plant with some of the features on the NPA4K mode.

The SSC-K code has also been used as the computational engine for the instrumentation and control system designer to study the detailed functioning of control modules by tracing their dynamic behavior, examining their parameters and algorithms. The detailed control system of KALIMER is being constructed.

2.6. Further Study for SSC-K Improvement

The SSC-L code has fairly generalized and detailed modeling of the plant protection system, and the plant instrument and control systems. However, these models need to be modified to be eligible for the KALIMER specific design. The SSC-K control system model is being developed

for design and analysis of the KALIMER control systems. The model is flexible, allowing the user to select any number of plant variables for input of the control system as measured quantities.

A sodium boiling model [13] for the analysis of the coolant boiling consequence from inception of boiling up to the time when the loss of fuel pin integrity is anticipated is being developed. If the coolant bulk temperature exceeds the saturation temperature by a user-specified amount of superheat, coolant boiling is assumed to be initiated, A vapor bubble is then generated at the place where the superheat criterion is met. The two-phase flow of transient liquid metal boiling in a narrow channel is characterized by use of the multiple-bubble slug flow approximation. Prediction of the typical phenomena is now possible, but sufficient validation on the calculation algorithm as well as the validity of the assumptions used in the model have not been made yet.

The SSC-K code has the following advantages compared to other system codes. SSC-K can be applied to both loop and pool-type LMR designs, whereas most systems codes are designed for only one reactor type. SSC-K can describe the hot pool in more detail than most of other system codes. The SSC-K code is now combined with the PSDRS module so that it does not require a sequence of other codes to calculate decay heat removal. SSC-K runs considerably faster than multi-dimensional system analysis codes.

The SSC-K code is being used for analyzing operational transients as well as safety analyses in the current KALIMER design, but the validity of the thermal hydraulic models in the SSC-K code should be confirmed for the pool plants. EBR-II tests have been used for the validation of the SSC-L which has loop type thermal hydraulics models. In the similar manner the PSDRS model in SSC-K also needs validation against data from a large scale experiment. Since there are no experimental data available for direct comparison to SSC-K in Korea, KAERI plans to compare the SSC-K code results with SASSYS-1 code [14].

3. ATWS Event Analyses

The models described in the previous sections have been implemented into SSC-K [2]. Using this version of SSC-K, KALIMER safety analyses for typical ATWS events have been performed to verify the logic of those models for reactivity, GEM, PSDRS, and pool thermal-hydraulics. Another purpose of the analyses is to evaluate the plant response, performance of certain inherent safety features, and the margin to plant safety limits. Although emphasis here is on the ATWS events for the safety analysis, SSC-K can be utilized for a variety of other objectives [15].

3.1. Description of KALIMER Plant

Currently, Korea is developing a conceptual design of KALIMER. The KALIMER concept provides enhanced safety margins and proliferation resistance. The safety advantages of the KALIMER reactor concept are derived from the use of sodium cooling, metallic fuel, and a pool configuration. These features lead to improve the heat transfer characteristics, reactivity feedback response, and passive safety capability. The reactor core, the four primary coolant pumps and the four IHXs are immersed in a large volume of sodium in the primary pool. The reactor vessel contains the entire inventory of primary sodium coolant. Fig. 9 shows the schematic of the KALIMER conceptual design.

The KALIMER core system [16] is designed with an 18-month refueling cycle. The core utilizes a heterogeneous configuration in the radial direction that incorporates annular rings of the internal blanket and driver fuel assemblies. The core layout

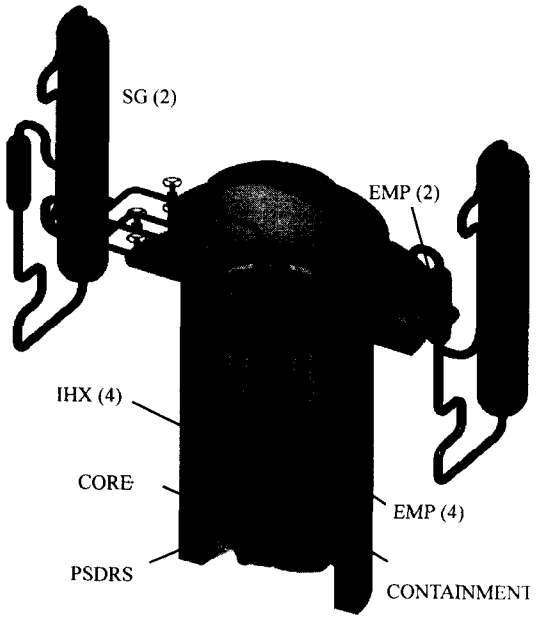

Fig. 9. Schematic of the KALIMER Design

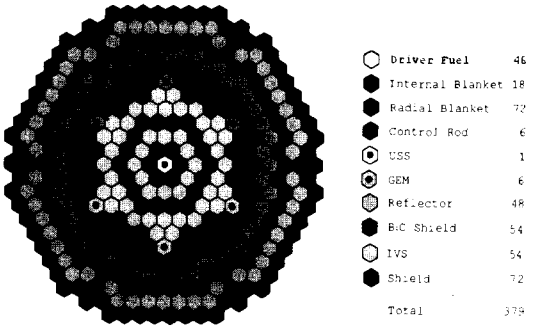

Fig. 10. KALIMER Breeder Core

is shown in Fig. 10. There are no upper or lower axial blankets surrounding the core. The active core height is 120.0 cm and the core outer diameter of all assemblies is 344.3 cm. The base alloy, ternary (U-Pu-10% Zr) metal fuel is used as the driver fuel. The fuel pin is made of sealed HT-9 tube containing metal fuel slug in columns. The fuel is immersed in sodium for thermal bonding with the cladding. A fission gas plenum is located above the fuel slug and sodium bond.

As shown in Fig. 10, the core includes 1 ultimate shutdown system (USS) assembly and 6 gas expansion modules (GEMs). For a safety margin in the event of loss of primary coolant flow, GEMs are located at the periphery of the active core. A GEM has the same external size and configuration as the ducts of the other core assemblies. As shown in Fig. 6, when the pumps are operating, sodium is pumped into the GEM, and the trapped helium gas is compressed into the region above the active core. In contrast, when the pumps are off, the helium gas region expands into the active core region, displacing the sodium in the GEM below the active core top. The resultant void near the core periphery increases neutron leakage and introduces significant negative reactivity.

The USS is included as a means to bring the reactor to a cold critical condition in the event of a complete failure of the normal scram system. The inherent reactivity feedback brings the core to a safe, but critical state at an elevated temperature. For this purpose the USS is located in the core center which drops the neutron absorber by gravity.

3.2. ATWS Events

The main analyses that are considered are the unprotected transient over power (UTOP), the unprotected loss of flow (ULOF), and the unprotected loss of heat sink (ULOHS). The UTOP is initiated due to insertion of reactivity in events such as withdrawal of control rods. The ULOF occurs due to a loss of power to the primary sodium pumps. The ULOHS results from a loss of the IHTS heat transfer function. For all of the unprotected events, evaluation of reactivity feedback is a major consideration. In that case, if feedwater to the steam generators is lost, the

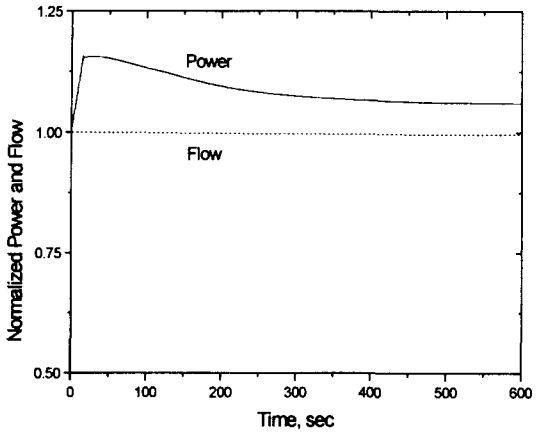

Fig. 11. Power and Flow (UTOP)

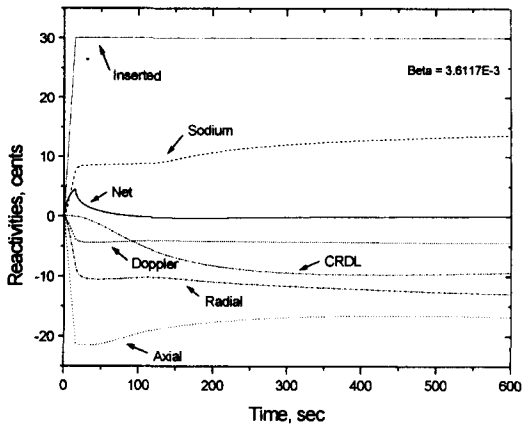

Fig. 12. Reactivity (UTOP)

assessment of the decay heat removal by PSDRS is then important.

The UTOP is assumed to insert 2 cents per second for 15 seconds, for total of 30 cents, representing the withdrawal of control rods. It is assumed that the primary and secondary sodium flows remain at the rated conditions and the feedwater is sufficient to keep the sodium outlet temperature from the steam generator constant. The UTOP transient results for power and flow, reactivity feedback and temperature are shown in Figs. 11 through 13. The general trends of these parameters are similar to those for a typical UTOP event. The power reaches a peak of 1.16 times the rated power and begins to level off at 1.06 times the rated power by 6 minutes, as shown in Fig. 11. The changes in the reactivity are shown in Fig. 12. The net reactivity starts out as a positive value because of the control rods being removed. The rise in fuel temperature first increases the Doppler absorption of the neutrons and then triggers fuel elongation. Higher sodium temperature leads to a harder neutronic spectrum, which generates a positive reactivity feedback. The higher sodium temperatures cause the thermal expansion of the control rod driveline and radial expansion, which are negative feedbacks. The control rod drivelines (CRDL) have a large time constant and are slow to act compared to radial expansion. The predicted fuel temperature distribution from the SSC-K code for the eighth axial fuel node from bottom of the hot driver is shown in Fig. 13. The peak temperatures of fuel (815 ℃), cladding (580 ℃), and sodium (580 ℃) are below the safety criteria [17] of KALIMER, individually.

For a loss of flow accident, the power to flow ratio is the key parameter that determines the consequences of the accident. Thus, the pump coastdown plays an important role in plant safety. The coastdown curve of the KALIMER pump has been directly embedded into the SSC-K code as function of flow vs time. The power transients during the ULOF are plotted in Fig. 14. For the case with GEMs, the power immediately begins to drop and reaches a decay heat level since there is enough negative reactivity insertion due to GEMs. Without the GEMs, the power is higher and decreases somewhat slowly. The fuel temperature distribution in the hot pin with the GEMs is shown in Fig. 15. The reduction of core flow due to the pump trips causes an initial peak centerline

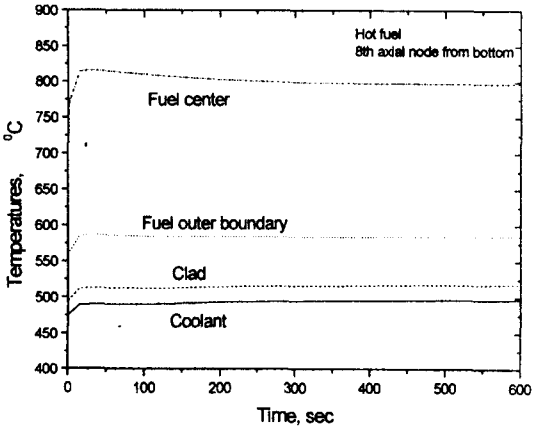

Fig. 13. Fuel Temperature (UTOP)

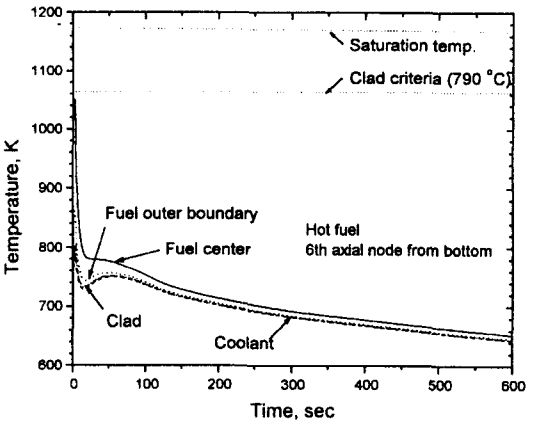

Fig. 15. Fuel Temperature (ULOF)

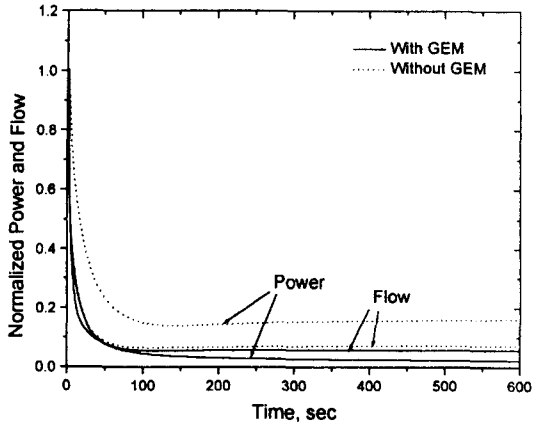

Fig. 14. Power and Flow Fraction (ULOF)

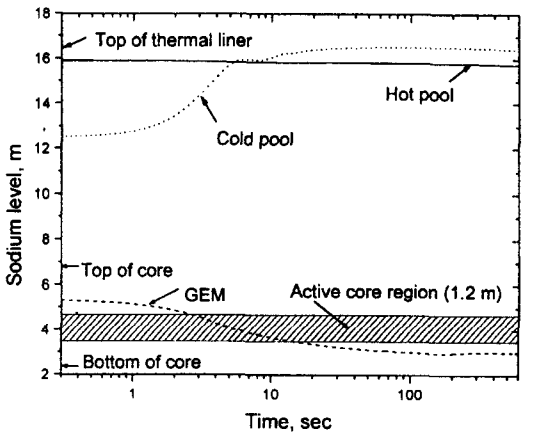

Fig. 16. Sodium Level (ULOF)

temperature before the power begins to fall. However, the peak fuel temperatures satisfy the safety criteria and ultimately the fuel temperatures decrease. The sodium levels for the pools and the GEM are shown in Fig. 16, where the cold pool level increases rapidly due to the pump trip, and it overflows the top of the reactor baffle, which is a divider for the cold and hot pools. The SSC-K well predicts the typical behavior of the core and system during a ULOF.

The ULOHS is assumed to begin with a sudden loss of the normal heat sink by the IHTS and steam generators. The only heat removal is available by the PSDRS. No plant protection system is assumed to be actuated during this transient; the pumps continue to run, and the power level is determined by inherent reactivity feedback. When the sodium heats up it expands and spills from the hot pool, over the top of the reactor baffle, down the vessel wall, and into the cold pool, bypassing the IHX. This direct contact of hot pool sodium on the vessel wall increases the

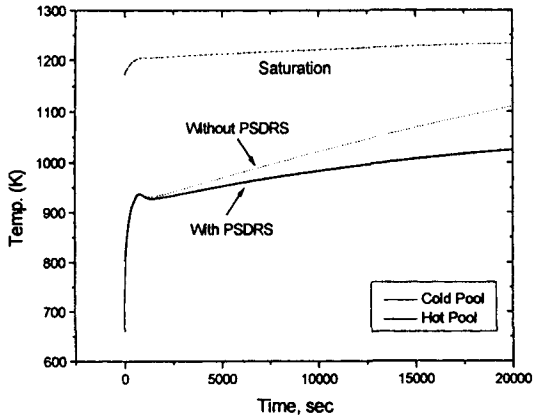

Fig. 17. Pool Temperature (ULOHS)

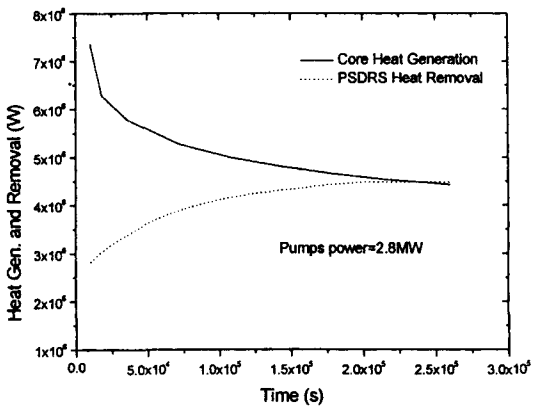

Fig. 18. Lont-term Heat Balance (ULOHS)

PSDRS heat removal rate. The loss of cooling in the IHX results in a rapid increase of the cold pool temperature within a short time. As illustrated in Fig. 17, the cold pool temperature reaches almost the same value as that in the hot pool within about 500 sec and so does the core inlet temperature. Thereafter, the temperature increases very slowly because of the large heat capacity of sodium in the pool as well as PSDRS heat removal. About 120 ℃ is estimated for the subcooling margin at 40,000 sec, based on the extrapolation of the temperature increase in Fig. 17. On the other hand, the increasing rate of the pool temperature without PSDRS is faster than that of the case with PSDRS by almost two times.

Fig. 18 shows the heat balance between core power generation and PSDRS heat removal. The core power decreases to the decay heat levels at about 800 seconds and is not affected by reactivity feedback thereafter. However, the thermal power of the four pumps corresponding to 2.8 MW is added to the core power throughout the entire transient, and the power generation rate drops below the PSDRS heat removal rate after long time of about 6.4 hours. Fig. 19 indicates the temperature contour in the hot pool at 150 seconds when the two-dimensional hot pool model is used. The maximum temperature difference in the hot pool is predicted to be 34 ℃.

4. Summary

The SSC-K code contains the models and features required for a pool-type reactor vessel and metallic fueled core. Reactivity feedback models of SSC-K code for Doppler, sodium density, fuel axial expansion, core radial expansion, and control rod driveline expansion effects produce physically consistent results, which show that the code is capable of modeling the phenomena properly. Physically consistent results are also obtained in the pool behaviors including variations of sodium level and temperature in the pools under the ATWS event conditions.

The results are presented to illustrate typical applications in the analysis of inherent safety. Although the analysis is preliminary in nature, it has been shown that the KALIMER design has inherent safety characteristics and is capable of accommodating ATWS events. The self-regulation of power without scram is mainly due to the inherent and passive reactivity feedback. The GEM

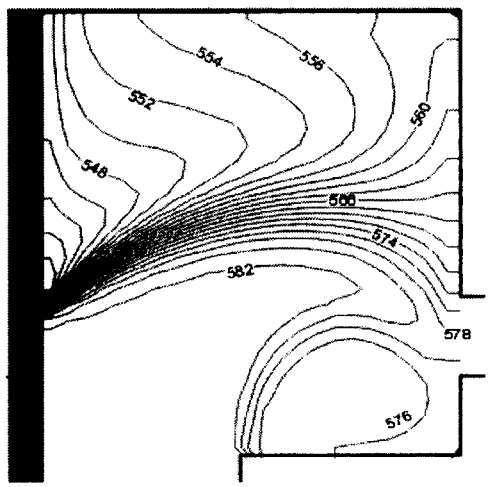

Fig. 19. Temperature Profile in the Hot Pool at 150s (ULOHS)

effect during ULOF appears to be highly effective. The preliminary analysis results show that the models implemented in the SSC-K work properly in a qualitative sense. However, the code validation and further investigation have to be made in order to utilize in the KALIMER design application.

Acknowledgements

This work was performed under the long-term nuclear research and development program sponsored by the Korea Ministry of Science and Technology.

Nomenclature

ρ_H Density of sodium in the hot pool (Kg/m^3)
A_{HP} Hot pool effective area (m^2)
Z_H Hot pool sodium level (m)
W_C Core sodium coolant flow (Kg/s)
$\Delta P_{f,g}$ Pressure losses due to friction and geometric change (Pa)
E_A Internal Energy in the upper mixing zone in the hot pool (J)
E_B Internal Energy in the lower mixing zone in the hot pool (J)
Q_{wall} Heat transfer rate between heat structure and sodium in the hot pool (W)
Q_{cgas} Heat transfer rate between sealing gas and sodium in the hot pool (W)
$Q_{interface}$ Heat transfer at interface between the upper and lower mixing zone (W)
$\frac{dz_j}{d_t}$ Interface velocity between the upper and lower mixing zone (m/s)
ρ_{cp} Density of sodium in the cold pool (Kg/m^3)
V_{cp} Voume of sodium in the cold pool (m^3)

References

1. Suk, S. D. and Park, C. K., "Conceptual Safety Design Analyses of Korea Advanced Liquid Metal Reactor," J. of Korean Nuclear Society, 31(6), 66-82 (1999).
2. Y. M. Kwon et al., "SSC-K Code User' s Manual (Rev.0)," KAERI/TR-1619/2000, Korea Atomic Energy Research and Institute (2000).
3. J. G. Guppy, "Super System Code (SSC, Rev.0) An Advanced Thermo-hydraulic Simulation Code for Transient in LMFBRs," NUREG/CR-3169 (1983).
4. Y. B. Lee et al., "Development of Two-Dimensional Hot Pool Model," KAERI/TR-1566/2000, Korea Atomic Energy Research and Institute (2000).
5. J. Zhu, "A Low-Diffusive and Oscillation Free Convection Schemes," Communications in Applied Numerical Methods, 7, 225-232 (1991).
6. J. P. Van Doormal and G. D. Raithby, "Enhancements of the SIMPLE Method for Predicting Incompressible Fluid Flows," Numerical Heat Transfer, 7, 147-163 (1984).

7. D. Hahn et al., "Reactivity Feedback Models for SSC-K," KAERI/TR-1105/98, Korea Atomic Energy Research and Institute (1998).
8. D. Hahn et al., "Inherent Safety Evaluation Models of SSC-K Code," Proceedings of the KNS, Seoul (October 1998).
9. W. P. Chang et al., "Development of the PSDRS Model for the KALIMER System Analysis Code SSC-K," KAERI/TR-1143/98, Korea Atomic Energy Research and Institute (1998).
10. W. P. Chang et al., "Development of the PSDRS Model for the KALIMER System Analysis Code SSC-K," Proceeding of the KNS, Seoul (October 1998).
11. G. J. Van Tuyle et al., "MINET Code Documentation," NUREG/CR-3668 (1989).
12. Y. B. Lee et al., "Development of NPA4K (Nuclear Plant Analyzer for KALIMER) Program," KAERI/TR-1567/2000, Korea Atomic Energy Research and Institute (2000).
13. W. P. Chang et al., "Development of Two-phase Flow Model, 'SOBOIL' for Sodium," KAERI/TR-1580/2000, Korea Atomic Energy Research and Institute (2000).
14. F. E. Dunn et al., "The SASSYS-1 LMFBR Systems Analysis Code," Proc. Int. Topical Meeting on Fast Reactor Safety, CONF-850410 (1985) 999-1006.
15. D. Hahn et al., "Preliminary Safety Analysis for Key Design Features of KALIMER," KAERI/TR-1616/2000, Korea Atomic Energy Research and Institute (2000).
16. D. Hahn et al., "KALIMER Preliminary Conceptual Design Report," KAERI/TR-1636/2000, Korea Atomic Energy Research and Institute (2000).
17. Y. M. Kwon, "Safety Related Design Bases Events," KALIMER/SA120-SB-01/99, Rev.1, Korea Atomic Energy Research and Institute (1999).